

The solutions to Eq. (A7) determine the class of quantum states for which the equivalence of quantum and semiclassical descriptions obtains. An obvious solution is

$$f(t) = e^{i\phi}, \quad (\text{A8})$$

or

$$g(n) = (n!)^{-1/2} N^{n/2} e^{-N/2} e^{i\phi}, \quad (\text{A9})$$

which defines the coherent states, as can be seen by comparison with (3.4). We shall now show that this solution is unique. This can *not* be done by expanding the right-hand side of (A7) in a power series and equating the coefficients of N^t on both sides. The reason is that $f(t)$ may itself be a function of N . We proceed instead by rewriting (A7) as

$$\sum_{t=0}^{\infty} \frac{N^t}{t!} f(t+r+\mu) f^*(t+r+\nu) = e^N, \quad (\text{A10})$$

where r , μ , and ν are arbitrary non-negative integers. Then we multiply both sides of the equation by

$(-N)^r/r!$ and sum over r ,

$$\sum_{r=0}^{\infty} \frac{(-N)^r}{r!} \sum_{t=0}^{\infty} \frac{N^t}{t!} f(t+r+\mu) f^*(t+r+\nu) = 1. \quad (\text{A11})$$

Next we make the change of variables $t = s - r$, and invert the order of summation,

$$\sum_{r=0}^{\infty} \sum_{s=r}^{\infty} = \sum_{s=0}^{\infty} \sum_{r=0}^s, \quad (\text{A12})$$

to obtain

$$\sum_{s=0}^{\infty} N^s f(s+\mu) f^*(s+\nu) \sum_{r=0}^s \frac{(-1)^r}{r!(s-r)!} = 1. \quad (\text{A13})$$

The sum over r is unity for $s=0$, and it is the binomial expansion of $(1-1)^s/s! = 0$ for $s > 0$, so that

$$f(\mu) f^*(\nu) = 1. \quad (\text{A14})$$

Since μ and ν are arbitrary, the solution is $f(t) = e^{i\phi}$ with ϕ constant.

Regge-Pole Models for High-Energy πN , KN , and $\bar{K}N$ Scattering*

ROGER J. N. PHILLIPS†

Lawrence Radiation Laboratory, University of California, Berkeley, California

AND

WILLIAM RARITA

752 Grizzly Peak Boulevard, Berkeley, California

(Received 27 April 1965)

It is shown that πN , KN , and $\bar{K}N$ elastic-scattering and charge-exchange data at high energy and small momentum transfer can be well fitted by assuming that the amplitudes are dominated by a few Regge poles in the crossed channel. The constraints imposed by the factorization principle are included. Unitary symmetry (SU_3) is approximately satisfied. Sample predictions of πp polarization and $K^+ + n \rightarrow K^0 + p$ charge exchange are made.

1. INTRODUCTION

THIS paper shows that the present pion-nucleon and kaon-nucleon data, at high energy and small momentum transfer, are consistent with the dominance of a few Regge poles in the crossed channel. Explicit models are constructed which give good fits to the data in the range of incident momentum 6 to 20 GeV/ c and squared momentum transfer $|t| < 1$ (GeV/ c)². Possible branch points in the complex angular-momentum plane are neglected. Mandelstam¹ has shown that such branch

points are probably not negligible at asymptotic energies; however, there seems to be a good chance that over a considerable energy range—perhaps up to 100 GeV or more—their effects are not important.²

There have already been several Regge-pole models^{3,4} (some including a cut^{5,6}) for the pion-nucleon and kaon-nucleon systems. However, the authors have not included the helicity-flip terms, have largely ignored the question of isospin dependence, and have not at-

² G. F. Chew and V. L. Teplitz, *Phys. Rev.* **136**, B1154 (1964).

³ A. Ahmadzadeh and I. A. Sakmar, *Phys. Rev. Letters* **11**, 439 (1963).

⁴ T. O. Binford and B. R. Desai, *Phys. Rev.* **138**, B1167 (1965).

⁵ P. G. O. Freund and R. Oehme, *Phys. Letters* **5**, 353 (1963).

⁶ I. R. Gatland and J. W. Moffat, *Phys. Rev.* **132**, 442 (1963); *Phys. Letters* **8**, 359 (1964).

* Work done under auspices of the U. S. Atomic Energy Commission.

† Permanent address: A. E. R. E., Harwell, Berkshire, England.

¹ S. Mandelstam, *Nuovo Cimento* **30**, 1127, 1148 (1963).

tempted accurate numerical fits to all the data. Also, high-energy charge-exchange measurements⁷⁻⁹ have not been made until recently, and are not considered in these earlier works.¹⁰

A characteristic of Regge-pole models is that the forward-scattering ("diffraction") peak shrinks with increasing energy when a single pole dominates. Proton-proton diffraction shrinks at present accelerator energies, but pion-nucleon and kaon-nucleon scattering show little or no effect¹¹; and this has sometimes been taken as evidence against Regge poles. However, in the range considered here there is no question of a single pole dominating; at least three poles are needed to explain the pion-nucleon data and five for the kaon-nucleon data. Various authors^{8,5,12,13} have shown that when several poles are significant the shrinking effect may be enhanced or even reversed. In the models which we construct below there is little shrinking for elastic scattering, partly because of secondary poles and partly because the slopes of the trajectories are not large. In πN charge exchange, however, a single pole is operative: Here we expect shrinking to be seen, and indeed the data show this effect, as already reported by Logan.¹⁰

Another important characteristic of Regge poles is the "signature factor," which fixes the phase of each pole contribution in terms of its energy dependence. The phase of the scattering amplitude in a Regge pole is thus fairly well determined by other aspects of the fit to data. When this phase can be measured directly, it offers a stringent test of the model. For the πN system this phase is known for forward elastic and charge-exchange scattering; for the $\bar{K}N$ system it is somewhat less well known; in all cases our models make satisfactory predictions (see Sec. 6). This is further evidence to support the Regge-pole hypothesis.^{14,15}

In Sec. 2 we describe the Regge poles that are used,

⁷ P. Astbury, G. Finocchiaro, A. Micheli, C. Verkerk, D. Websdale, C. West, W. Beusch, B. Gobbi, M. Pepin, M. Ponchon, and E. Polgar, *Proceedings of the Twelfth Annual International Conference on High Energy Physics, Dubna, 1964* (Atomizdat, Moscow, 1965).

⁸ A. V. Stirling, P. Sonderegger, J. Kirz, P. Falk-Vairant, O. Guisan, C. Bruneton, P. Borgeaud, M. Yvert, J. P. Guillaud, C. Caverzasio, and B. Amblard, *Phys. Rev. Letters* **14**, 763 (1965); J. Kirz (private communications).

⁹ I. Mannelli, A. Bigi, R. Carrara, M. Wahlig, and L. Sodickson, *Phys. Rev. Letters* **14**, 408 (1965).

¹⁰ R. K. Logan, *Phys. Rev. Letters* **14**, 414 (1965), has recently analyzed the charge-exchange data of Ref. 9 using one Regge pole; however, he does not include elastic scattering or total cross sections.

¹¹ K. J. Foley, S. J. Lindenbaum, W. A. Love, S. Ozaki, J. J. Russell, and L. C. L. Yuan, *Phys. Rev. Letters* **11**, 425, 503 (1963).

¹² R. J. N. Phillips, *Phys. Letters* **5**, 159 (1963).

¹³ B. R. Desai, *Phys. Rev. Letters* **11**, 59 (1963).

¹⁴ The asymptotic phase of a Regge-pole contribution follows from its simple power-law dependence on energy, as shown by dispersion relations (e.g., Refs. 10 and 15). So the part of the Regge pole hypothesis that is being tested here is the assumption that the complete amplitude is a sum of a few terms, each proportional to a power of the energy, and each having a simple isospin and G parity in the crossed channel. This is a nontrivial assumption.

¹⁵ A. Bialas and E. Bialas, *Nuovo Cimento* **37**, 1686 (1965).

the forms of the scattering amplitudes, and our particular parametrizations of trajectories and residue functions. Within this framework there is no unique set of parameters that fits the data. We have found several kinds of solution, which are illustrated.

Section 3 concerns the "crossover" effect: The differential cross section for $\pi^\pm p$ scattering intersect in the small-momentum-transfer region, and thereby pose a problem for Regge-pole fitting. $K^\pm p$ scattering shows the same effect. One of the main differences between our various models is how they explain this phenomenon.

The factorization principle relates the residue functions of a given Regge pole in different physical amplitudes, as described in Sec. 4. These constraints have been included in our models.

In Sec. 5 we discuss the relations implied by the unitary symmetry group SU_3 . These are ignored in the process of fitting the data, but are approximately satisfied by the results.

The experimental data and the method of fitting parameters are described in Sec. 6.

Various fits to the data are summarized, illustrated, and discussed in Sec. 7. A partial-wave analysis of some typical solutions is given, to be compared to other models that have been proposed, and to show that the unitary bound is respected. The ratio of real to imaginary part of the forward-scattering amplitude is compared to experiment. Some predictions of high-energy πN polarization and $K^+n \rightarrow K^0 p$ charge exchange are made.

2. FORMALISM

Consider first πN scattering. Then at least three Regge poles are needed to fit the data. The Pomeranchuk pole P describes the asymptotic limit; a second vacuum pole P' and the ρ pole are needed to give the differences of $\pi^\pm p$ amplitudes from the asymptotic limit and from each other. We take just these three.

Singh¹⁶ among others has described the Regge-pole formalism for this case. There is a helicity-flip amplitude B and a nonflip amplitude A (which Singh calls A'), in terms of which the total and differential cross sections are

$$\sigma_T(s) = \text{Im}A(s, t=0)/p, \quad (1)$$

$$\frac{d\sigma}{dt}(s, t) = \frac{1}{\pi s} \left(\frac{m_N}{4k} \right)^2 \left\{ \left(1 - \frac{t}{4m_N^2} \right) |A|^2 + \frac{t}{4m_N^2} \left(s - \frac{s+p^2}{1 - (t/4m_N^2)} \right) |B|^2 \right\}. \quad (2)$$

Here s and t are the invariant squares of energy and

¹⁶ V. Singh, *Phys. Rev.* **129**, 1889 (1963).

momentum transfer, p is the pion lab momentum, k is the c.m. momentum, and m_N is the nucleon mass.

Each pole gives to A and B terms of the form

$$\begin{aligned} A_i &= -C_i(\exp(-i\pi\alpha_i) \pm 1/\sin\pi\alpha_i)(E/E_0)^{\alpha_i}, \\ B_i &= -D_i(\exp(-i\pi\alpha_i) \pm 1/\sin\pi\alpha_i)(E/E_0)^{\alpha_i-1}, \end{aligned} \quad (3)$$

in a high-energy approximation. Here the label i denotes P , P' or ρ , $\alpha_i(t)$ is the trajectory, $E = (p^2 + m_\pi^2)^{1/2}$ is the total pion lab energy, and E_0 is an arbitrary scale parameter, which we take for convenience to be 1 GeV. The sign \pm in the signature factor is $+$ for P and P' but $-$ for ρ . $C_i(t)$ and $D_i(t)$ are real functions related to the pole residues. When units $\hbar=c=1$ are used, A_i and C_i have the dimension (length), B_i and D_i have the dimension (length)².

For definiteness, let the contributions A_i and B_i defined above refer to π^-p scattering. Then the various πN amplitudes of present interest have the forms

$$A(\pi^- + p \rightarrow \pi^- + p) = A_P + A_{P'} + A_\rho, \quad (4)$$

$$A(\pi^+ + p \rightarrow \pi^+ + p) = A_P + A_{P'} - A_\rho, \quad (5)$$

$$A(\pi^- + p \rightarrow \pi^0 + n) = -\sqrt{2}A_\rho. \quad (6)$$

The helicity-flip amplitudes are similarly related.

Consider now KN and $\bar{K}N$ scattering. Regge poles in this context have been discussed by Sakmar.¹⁷ Besides the poles already described, two more poles with negative G parity (which cannot affect πN) are needed to fit the total cross-section data.¹⁸ These are the ω pole (in which we include any contribution from the nearby ϕ pole) and the R pole proposed by Pignotti.^{19,20} The argument for an R term in kaon-nucleon scattering is given in Ref. 21.

Just as for πN scattering, there are two amplitudes for each process and the pole terms have the same forms as in Eqs. (3). The various amplitudes of present interest have the forms

$$A(K^- + p \rightarrow K^- + p) = A_P + A_{P'} + A_\omega + A_\rho + A_R, \quad (7)$$

$$A(K^- + n \rightarrow K^- + n) = A_P + A_{P'} + A_\omega - A_\rho - A_R, \quad (8)$$

$$A(K^+ + p \rightarrow K^+ + p) = A_P + A_{P'} - A_\omega - A_\rho + A_R, \quad (9)$$

$$A(K^+ + n \rightarrow K^+ + n) = A_P + A_{P'} - A_\omega + A_\rho - A_R, \quad (10)$$

$$A(K^- + p \rightarrow \bar{K}^0 + n) = 2A_\rho + 2A_R, \quad (11)$$

$$A(K^+ + n \rightarrow K^0 + p) = -2A_\rho + 2A_R. \quad (12)$$

We come now to the parametric forms assumed for the α_i , C_i , and D_i .

¹⁷ Ismail A. Sakmar, thesis, Lawrence Radiation Laboratory Report UCRL-10834, May 1963.

¹⁸ W. Galbraith, E. W. Jenkins, T. F. Kycia, B. A. Leontic, R. H. Phillips, A. L. Read, and R. Rubinstein, *Proceedings of the Twelfth Annual International Conference on High Energy Physics Dubna, 1964* (Atomizdat, Moscow, 1965).

¹⁹ A. Pignotti, *Phys. Rev.* **134**, B630 (1964).

²⁰ A. Ahmadzadeh, *Phys. Rev.* **134**, B633 (1964).

²¹ R. J. N. Phillips and W. Rarita, *Phys. Rev.* **138**, B723 (1965).

In the range considered, data fitting is not very sensitive to the form of the trajectories $\alpha_i(t)$. Probably straight lines would suffice, but we have used a two-parameter form suggested by Pignotti²² which includes some curvature:

$$\alpha(t) = -1 + [1 + \alpha(0)]^2 / [1 + \alpha(0) - \alpha'(0)t]. \quad (13)$$

The two parameters are $\alpha(0)$ and $\alpha'(0)$, the value and slope at $t=0$.

For the residue functions $C_i(t)$ and $D_i(t)$, the data suggest something approximately exponential in the small- t region, decreasing less strongly at larger values of t . The data we seek to fit lie mostly in the former region. Accordingly, for the even-signature poles P , P' , and R we generally take the empirical forms

$$C(t) = C_0\alpha(t)[2\alpha(t)+1] \exp(C_1t), \quad (14)$$

$$D(t) = D_0\alpha(t) \exp(D_1t). \quad (15)$$

In a few cases $\exp(C_1t)$ in Eq. (14) is replaced by $\exp(C_1t + C_2t^2)$. The factors $(2\alpha+1)$ in $C(t)$ and $\alpha(t)$ in $D(t)$ are angular-momentum weight factors; the factor $\alpha(t)$ in $C(t)$ is to remove the unphysical singularity ("ghost state") that would otherwise occur, when and if the trajectory passes through $\alpha=0$ in the region $t < 0$.

For the odd-signature poles ρ and ω , the crossover phenomenon (see Sec. 3) suggests that the residue functions may change sign. For this possibility we use a difference of exponentials.

$$C(t) = C_0\alpha(0)[2\alpha(t)+1][(1+G) \exp(C_1t) - G \exp(C_2t)], \quad (16)$$

$$D(t) = D_0\alpha(t)[(1+H) \exp(D_1t) - H \exp(D_2t)]. \quad (17)$$

In the limit $G=0$, Eq. (16) reduces to Eq. (14), except that the ghost-killing factor (not needed for odd signature) is replaced by the constant $\alpha(0)$. For $H=0$, Eq. (17) reduces to Eq. (15). Another way to parameterize a sign change is to multiply a single exponential by a factor $(t-t_0)$; we tried this but found Eqs. (16) and (17) more satisfactory.

The parameterizations above are intended only for the range under discussion, $0 \leq |t| < 1$ (GeV/c)². It is not suggested that they can be extrapolated as they are beyond this range. They are purely empirical.

3. CROSSOVER EFFECT

Near $t=0$ the π^-p differential cross section is slightly greater than the π^+p value, at each energy. For larger t , however, the π^+p cross section is greater. The crossover point seems to lie near $t = -0.05$ (GeV/c)². This effect has special implications for the ρ pole.

It is natural to suppose first that the nonflip amplitude A dominates at small t and is responsible for the crossover effect. Then the $\pi^\pm p$ cross-section difference

²² A. Pignotti, *Phys. Rev. Letters* **10**, 416 (1963).

is due to the interference term between $(A_P + A_{P'})$ and A_ρ . Since this interference term changes sign at the crossover, either A_ρ changes sign or the relative phase passes through $\pm\pi/2$. However, in a Regge-pole model the phase of each term is tied to its energy dependence, and it can be shown that in our case this relative phase cannot approach $\pm\pi/2$ for small t . Hence, if A_ρ dominates the crossover, it must change sign.

Now in fact the amplitude B_ρ is not negligible at the crossover point. If it were, the $\pi^- + p \rightarrow \pi^0 + n$ charge-exchange cross section would vanish, whereas nothing of the kind happens.

If we include a substantial B_ρ effect, A_ρ can still explain the crossover by changing sign, but an alternative explanation also appears. Suppose that the interference term between $(B_P + B_{P'})$ and B_ρ is rather strong, and that it has the opposite sign to the interference between $(A_P + A_{P'})$ and A_ρ . Then at $t=0$ the $\pi^\pm p$ cross-section difference is given by the A term, since there is no helicity-flip contribution here. However, as $|t|$ increases the B term can overtake the A term and reverse the cross-section difference.

We thus have two simple explanations: (a) A_ρ changes sign, (b) A_ρ and B_ρ effects have opposite sign, but neither goes through zero. Of course other explanations can be constructed by combining or modifying (a) and (b). For instance, (c) A_ρ and B_ρ effects have opposite signs and A_ρ goes through zero, (d) A_ρ and B_ρ both change sign, at different values of t , etc.

A similar but stronger crossover seems to occur with the $K^\pm p$ differential cross sections. Though we have no small-angle $K^- p$ data, the total cross sections with the optical theorem suggest the forward cross section is greater for $K^- p$; in our model this is certainly so. At larger angles, however, the $K^+ p$ value becomes much the larger, by a factor of 2 or more. In our models the crossover must be due to the ρ and ω poles. The same general types of explanation can be constructed as in the πN case, subject to certain constraints. If A_ω changes sign, then so does B_ω (see Sec. 4). The total cross-section data also require both A_ω and A_ρ to have the same sign at $t=0$.

Because the $K^\pm p$ crossover is a bigger effect, it is harder to fit the data purely by a helicity-flip effect of type (b) than in the case of the $\pi^\pm p$ crossover. A good fit seems to require a sign change in a residue function (see Sec. 7).

4. FACTORIZATION CONSTRAINTS

The factorization theorem of Gell-Mann²³ and Gribov and Pomeranchuk²⁴ states that the πN residue functions have the forms

$$C_i(\pi N) = E_0 \eta_{\pi i} [\eta_{1i} + \eta_{2i} t / (4m_N^2 - t)], \quad (18)$$

$$D_i(\pi N) = \eta_{\pi i} \eta_{2i}, \quad (19)$$

²³ M. Gell-Mann, Phys. Rev. Letters 8, 263 (1962).

²⁴ V. N. Gribov and I. Ya. Pomeranchuk, Phys. Rev. Letters 8, 343 (1962).

following the notation of Ref. 25, where E_0 is the same scale constant as in Eqs. (3); $\eta_{\pi i}$ characterizes the coupling of Regge pole i to the $\pi\pi$ system, while η_{1i} and η_{2i} give its coupling to the $\bar{N}N$ system. The KN residue functions are similar, with $\eta_{\pi i}$ replaced by $\eta_{K i}$.

This immediately gives a relation between the πN and KN terms:

$$A_i(\pi N)/B_i(\pi N) = A_i(KN)/B_i(KN) \quad (20)$$

for the Regge poles common to both problems, $i=P, P'$, and ρ .

The factor functions $\eta_{\pi i}$, $\eta_{K i}$, η_{1i} , and η_{2i} are usually assumed to be analytic and real in the scattering region of interest. Hence if $A_\rho(\pi N)$ changes sign near the crossover (Sec. 3), either $\eta_{\pi\rho}$ or $\eta_{1\rho}$ must change sign. It cannot be $\eta_{\pi\rho}$, since that would make both A_ρ and B_ρ vanish at the same point, giving zero charge exchange. So $\eta_{1\rho}$ must change sign. Hence $A_\rho(KN)$ also changes sign at the same point.

In the $N\bar{N}$ and $\bar{N}N$ problems, residue functions $(\eta_{1i})^2$, $(\eta_{2i})^2$, and $\eta_{1i}\eta_{2i}$ appear. Clearly there are many constraints, relating these to each other and to the πN and KN problems. Rarita and Teplitz^{26,27} have argued that the residue function corresponding to $(\eta_{1\omega})^2$ must change sign in order to explain a crossover effect between the $p\bar{p}$ and $\bar{p}p$ differential cross sections. Such a sign change would contradict the assumption of real analyticity for the η_i . However, the actual residue functions themselves would remain real in the example cited if $(\eta_{1\omega})^2$, $(\eta_{2\omega})^2$, $(\eta_{K\omega})^2$, and all the other squared ω -factor functions changed sign at the same point.

5. UNITARY SYMMETRY

The unitary symmetry group SU_3 gives several relations that are interesting to consider, even though the symmetry is not exact.²⁸

Now, π , K , and \bar{K} are supposed to belong to a common unitary octet; hence the $\pi\pi$ and $\bar{K}K$ couplings to a singlet, such as the Pomeranchuk pole P , should be equal:

$$\eta_{\pi P} = \eta_{K P}. \quad (21)$$

Hence $A_P(\pi N) = A_P(KN)$ and $B_P(\pi N) = B_P(KN)$. The same holds for P' , if it too is a unitary singlet.

The ρ pole belongs to an octet. The coupling between this particular octet and the $\pi\pi$ and $\bar{K}K$ octets must be pure F type to preserve charge-conjugation invariance.²⁹ Hence there is a precise relation between the couplings,

$$\eta_{\pi\rho} = 2\eta_{K\rho}, \quad (22)$$

²⁵ M. Gell-Mann, in *Proceedings of 1962 Annual International Conference on High-Energy Nuclear Physics at CERN*, edited by J. Prentki, (CERN, Geneva, 1962), p. 533.

²⁶ W. Rarita and V. L. Teplitz, Phys. Rev. Letters 12, 206 (1964).

²⁷ A similar conclusion is reached in Ref. 4.

²⁸ See, e.g., M. Gell-Mann, Phys. Rev. 125, 1067 (1962).

²⁹ H. Lipkin, Phys. Letters 7, 221 (1963).

where the relative sign is given to agree with the conventions of Eqs. (4)–(12) and (18), (19). Hence $A_\rho(\pi N) = 2A_\rho(KN)$ and $B_\rho(\pi N) = 2B_\rho(KN)$.

The ω pole we have introduced is meant to stand for both ω and ϕ , which belong partly to the same octet as ρ but partly also to a singlet. No useful relations concerning them can be inferred without further specific assumptions.

The R pole is supposed to belong to an octet and Pignotti¹⁹ suggested that the isoscalar member of this octet (let us denote it S) might in fact play the physical role usually ascribed to a second vacuum pole P' . Now this octet must have pure D -type coupling to the $\pi\pi$ and $\bar{K}K$ octets,²⁰ so we have

$$(1/\sqrt{3})\eta_{KR} = -\eta_{KS} = \frac{1}{2}\eta_{\pi S}. \quad (23)$$

This implies $A_S(\pi N) = -2A_S(KN)$ and $B_S(\pi N) = -2B_S(KN)$, and shows that Pignotti's suggestion about the role of S is untenable: S cannot substitute for P' , since total cross-section data require at least that $A_{P'}(\pi N)$ and $A_{P'}(KN)$ have the same sign at $t=0$. However, our empirical P' term may in fact include a contribution from S , and may, therefore, not behave like a pure singlet.

We cannot compare the complete R and S amplitudes, since we do not know the F/D ratio of their coupling to $\bar{N}N$.

6. DATA AND PARAMETER FITTING

The experimental data used are as follows. Total cross sections for $\pi^\pm p$, $K^\pm p$, and $K^\pm n$ at 6, 8, 10, 12, 14, 16, 18, and 20 GeV/ c are taken from Ref. 18. Elastic differential cross sections are taken from Ref. 11 for π^+p at 6.8, 8.8, 10.8, 12.8, 14.8, and 16.7 GeV/ c ; for π^-p at 7, 8.9, 10.8, 13, 15, 17, and 18.9 GeV/ c ; for K^+p at 6.8, 9.8, 12.8, and 14.8 GeV/ c ; and for K^-p at 7.2 and 9 GeV/ c . For $\pi^-+p \rightarrow \pi^0+n$ charge exchange, we use data from Ref. 9 at 6, 8, 10, 12, 14, and 16 GeV/ c and from Ref. 8 at 5.9, 9.8, 13.3, and 18.2 GeV/ c . Our $K^-+p \rightarrow \bar{K}^0+n$ data are at 9.5 GeV/ c , from Ref. 7. In all we use 334 πN data points, plus 115 more for KN and $\bar{K}N$; most of these are illustrated in the next section.

Recently fresh $\pi^\pm p$ differential cross-section measurements have been made³⁰ at 8.5, 12.4, and 18.4 GeV/ c . These results are very similar to those of Ref. 11, but there are small systematic differences which make it hard to fit both sets simultaneously. Accordingly we have chosen to omit the data of Ref. 30 from the final analysis.

The πN charge-exchange data of Ref. 8 show a minimum near $t = -0.6(\text{GeV}/c)^2$, followed by a slight

rise. It is not clear whether we should seek an explanation of this in terms of the ρ Regge pole. We therefore constructed two kinds of solution, one including and one excluding the charge-exchange data beyond this minimum.

The parameters of our models were optimized by least-squares fitting to data, using the IBM-7094 computers at the Lawrence Radiation Laboratory, with programs based on a variable metric minimization method.³¹ The parameters were also restricted to satisfy reasonable physical criteria. The coefficients C_1 , C_3 , D_1 , and D_3 appearing in exponentials [see Eqs. (14)–(17)] were not allowed to become negative, nor very large; a practical upper limit $(4m_\pi)^{-1} \approx 12.5 \text{ GeV}^{-2}$ was imposed. The zero intercept of the P trajectory was fixed at $\alpha_P(0) = 1$: Some empirical support for this choice is described in Sec. 7.

Perhaps the most important constraint we applied was unitarity. Each solution was decomposed numerically into partial waves and the partial amplitudes were compared with the unitary bound. Violations of unitarity were tolerated only if the partial amplitudes concerned were essentially zero and contributed nothing to the fit to data; we regard these marginal violations as being consequences of imperfect parameterization and having no physical significance. Substantial violations of unitarity were not tolerated; the corresponding solutions were modified and constrained until they conformed.

It is interesting to note the types of unitarity violation that occurred. We did not find the type most expected, in which the lowest partial amplitudes become too large, but we found two unexpected types. (i) To illustrate the first type, consider a spinless problem at some given energy, with a pure imaginary amplitude $i \exp(at)$. It can be shown that all the partial-wave amplitudes are positive imaginary, because of the special properties of Bessel functions. However, if instead the amplitude is $i \exp(at + bt^2)$, the partial amplitudes do not all have the same sign; some are negative imaginary and violate unitarity. We met this type of violation when the parameter C_2 was used [see below, Eq. (14)]; fortunately the offending terms were usually very small and in high angular-momentum states, and had no physical importance. This kind of violation seems clearly due to oversimplified parameterization of the amplitudes. (ii) To illustrate the second type, consider the usual "nonrelativistic" definition of nonflip and spin-flip amplitudes. For given orbital angular momentum L , the nonflip contribution contains a sum of partial amplitudes $(L+1)a_{L+} + La_{L-}$ and the spin-flip terms contains the difference $a_{L-} - a_{L+}$. Suppose the partial amplitudes $a_{L\pm}$ are imaginary: then for a fixed nonflip term, the spin-flip term cannot increase indefinitely without either a_{L+} or a_{L-} becoming negative

³⁰ D. Hartig, P. Blackall, B. Elsner, A. C. Helmholz, W. C. Middelkoop, B. Powell, B. Zacharav, P. Zanella, P. Dalpiaz, M. N. Focacci, S. Focardi, G. Giacomelli, L. Monari, J. A. Beany, R. A. Donald, P. Mason, L. W. Jones, and D. O. Caldwell, Nuovo Cimento (to be published).

³¹ W. C. Davidon, Argonne National Laboratory Report No. ANL-5990 (Rev.), 1959 (unpublished).

and violating unitarity. The relation of our amplitudes A and B to partial waves is more complicated,³² but we did find essentially this type of violation when B contributed too strongly to high partial waves; the remedy was to reduce and restrain the coefficients D_0 and D_1 [see Eq. (15)].

We began by fitting the πN data. With this analysis used to fix the ratios A/B (from factorization) and the trajectories $\alpha(t)$ for P , P' , and ρ , the KN and $\bar{K}N$ data were fitted by adjusting the remaining parameters.

The value of χ^2 , characterizing the goodness of fit to data, requires some comment. Ideally, with data free from systematic error and a perfect theory, the expected value is the number of data points less the number of adjusted parameters. However, when the quoted accuracy of data becomes less than the systematic errors of experiment or theory, the value of χ^2 soars. We found two places where this happens. Firstly, the K^+p total cross sections¹⁸ are given to ± 0.1 mb, and in the mean are almost constant with energy; however, there are some fluctuations of order 0.3 mb, so that no theory with a smooth energy variation can give a textbook fit. These eight points contribute typically about 23 to χ^2 . Secondly, the $\pi^- + p \rightarrow \pi^0 + n$ data from Ref. 8 show systematic deviations at small angles from the single-power energy dependence of our models; the apparent rate of change, comparing 5.9 and 18.2 GeV/ c data, is greater than that obtained by comparing 9.8 and 13.3 GeV/ c . The quoted uncertainty is as small as 3% for many points. As a result, the 40 data points with $|t| < 0.2$ (GeV/ c)² contribute typically about 100 to χ^2 . With data of such precision, even a small systematic divergence between theory and experiment has a big effect on χ^2 ; whether theory or experiment is at fault we cannot say. However, the charge-exchange data

have appreciable uncertainties in t , which we have not folded in.

7. RESULTS AND DISCUSSION

Four solutions are given in the tables. Table I lists the parameters $\alpha_i(0)$ and $\alpha_i'(0)$ of the trajectories (abbreviated to α_i and α_i'): $\alpha_P=1$ is not listed. Tables

TABLE I. Trajectory parameters. The slopes α' are in units (GeV/ c)⁻².

Solution	$\alpha_{P'}$	$\alpha_{P''}$	$\alpha_{P''}$	α_ρ	$\alpha_{\rho'}$	α_R	$\alpha_{R'}$	α_ω	$\alpha_{\omega'}$
1	0.34	0.50	0.34	0.54	0.65	0.32	0.80	0.52	0.60
2	0.34	0.50	0.34	0.53	0.71	0.30	0.55	0.50	0.60
3	0.34	0.50	0.34	0.54	0.78	0.30	0.75	0.52	0.60
4	0.34	0.50	0.34	0.53	0.75	0.31	0.55	0.52	0.60

II and III give the coefficients of the amplitudes $A_i(\pi N)$ and $B_i(\pi N)$, respectively. Table IV shows parameters that connect the KN and πN contributions from P , P' , and ρ , in the notation

$$A_i(KN)/A_i(\pi N) = B_i(KN)/B_i(\pi N) = F_0 \exp(F_1 t). \quad (24)$$

Table V gives the coefficients for the R and ω KN amplitudes.

The fit to data is illustrated in Figs. 1 through 7 for the typical case of solution 1.

Solution 1 explains the πN crossover effect both because A_ρ changes sign and by B_ρ interference; in terms of the discussion of Sec. 3, it is of type (c). The KN crossover is explained with the help of the change of sign A_ω . The dip and second maximum in πN charge exchange is explained because B_ρ goes through zero near $t = -0.6$ (GeV/ c)². The fit to 334 πN data, with

TABLE II. πN nonflip amplitude coefficients.

Solution	P		P'			ρ			G
	C_0 (mb \times GeV)	C_1 (GeV ⁻²)	C_0 (mb \times GeV)	C_1 (GeV ⁻²)	C_2 (GeV ⁻⁴)	C_0 (mb \times GeV)	C_1 (GeV ⁻²)	C_2 (GeV ⁻²)	
1	6.55	2.51	19.6	4.04	...	2.45	5.6	0.14	0.50
2	6.60	2.24	18.6	2.48	-10.3	2.61	9.6	0.00	0.47
3	6.52	2.58	20.0	4.01	...	2.45	11.4
4	6.58	2.44	18.9	2.24	-11.2	2.60	12.5

TABLE III. πN helicity-flip amplitude coefficients.

Solution	P		P'			ρ		H
	D_0 (mb)	D_1 (GeV ⁻²)	D_0 (GeV ⁻²)	D_1 (GeV ⁻²)	D_0 (mb)	D_1 (GeV ⁻²)	D_2 (GeV ⁻²)	
1	-7.5	0.51	-101	8.1	56.9	1.64	0.31	0.90
2	-6.5	0.65	69.5	2.50	0.59	0.51
3	-11.4	0.90	-101	8.1	62.4	3.17
4	-22.3	1.73	67.5	3.39

³² The relation is provided by combining Ref. 16 with G. Chew, M. Goldberger, F. Low, and Y. Nambu, Phys. Rev. **106**, 1337 (1957).

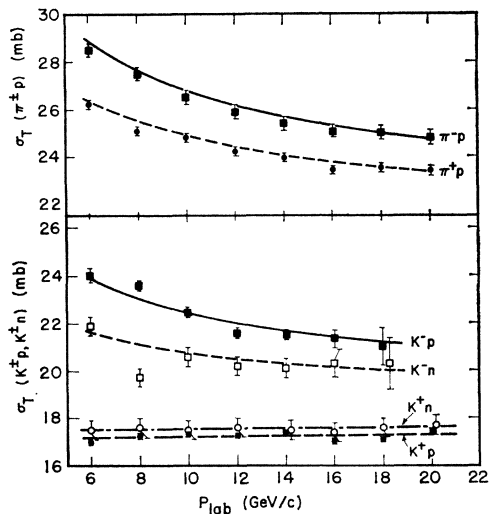


FIG. 1. Total cross sections for $\pi^\pm p$, $K^\pm p$, and $K^\pm n$ from Ref. 18, compared with solution 1.

21 adjustable parameters, has $\chi^2=504$. The fit to 115 KN data, with 18 parameters, has $\chi^2=152$.

Solution 2 gives essentially the same explanation for the crossover and charge-exchange effects. However, the $B_{P'}$ term—whose main role is apparently to give some convexity to the cross-section plots—is dropped and a factor $\exp(C_2 p^2)$ introduced in $A_{P'}$ instead. The fit to 334 πN points with 20 parameters has $\chi^2=482$. The fit to 115 KN points with 18 parameters has $\chi^2=139$.

Solution 3 explains the πN crossover by B_p interference; in terms of Sec. 3, it is of type (b). A corresponding explanation for the KN crossover, adding B_ω interference effects, was tried but proved unsatisfactory. Accordingly, the KN crossover here relies on a change

TABLE IV. Parameters relating P , P' , and ρ contributions to πN and KN .

Solution	P		P'		ρ	
	F_0	F_1 (GeV^{-2})	F_0	F_1 (GeV^{-2})	F_0	F_1 (GeV^{-2})
1	0.901	-0.23	0.279	-1.61	0.527	0.01
2	0.896	-0.22	0.285	-1.19	0.521	0.01
3	0.905	-0.21	0.280	-1.72	0.529	0.01
4	0.900	-0.18	0.281	-1.27	0.480	0.00

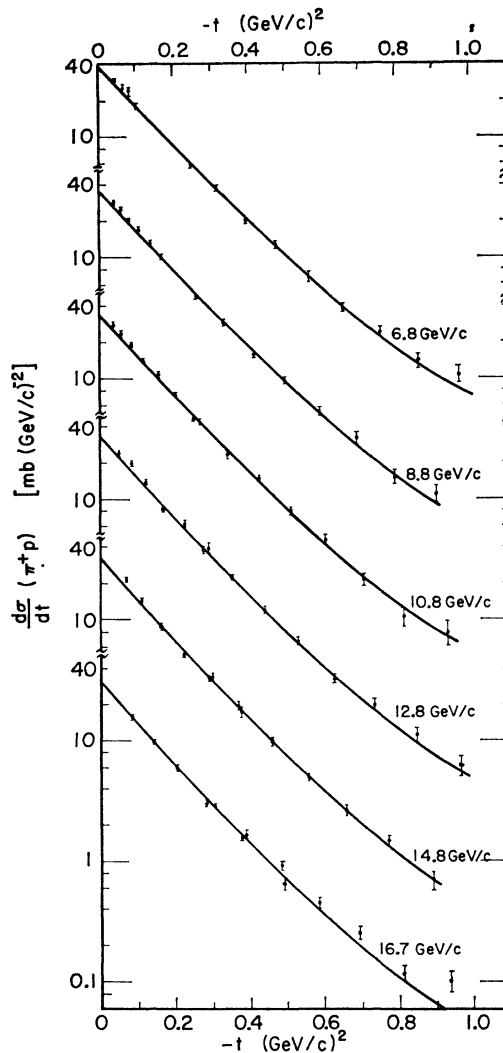


FIG. 2. $\pi^+ p$ differential cross sections at 6.8, 8.8, 10.8, 12.8, 14.8, and 16.7 GeV/c , from Ref. 11, compared with solution 1. The different sets are spaced by a decade.

of sign in A_ω , and B_ω is not used at all. Solution 3 contains no explanation for the second maximum in πN charge exchange: in making the fit, the data of Ref. 8 for $|t| > 0.6$ were omitted; $\chi^2=502$ for 322 πN points with 17 parameters; $\chi^2=155$ for all 115 KN points with 18 parameters.

TABLE V. KN amplitude coefficients for R and ω .

Solution	R				ω			G
	C_0 ($\text{mb} \times \text{GeV}$)	C_1 (GeV^{-2})	D_0 (mb)	D_1 (GeV^{-2})	C_0 ($\text{mb} \times \text{GeV}$)	C_1 (GeV^{-2})	C_2 (GeV^{-2})	
1	3.34	2.16	-31.2	1.76	5.99	10.5	0.17	0.86
2	3.69	2.81	-29.3	1.77	6.62	10.0	0.02	0.66
3	3.50	2.21	-32.2	1.73	6.14	10.0	0.27	0.99
4	3.71	2.83	-29.5	1.78	6.34	10.0	0.00	0.69

Solution 4 explains the crossover and ignores the second maximum in πN charge exchange in the same way as solution 3. However, like solution 2, it drops $B_{P'}$ and introduces a factor $\exp(C_2 t^2)$ in $A_{P'}$ instead. The fit to 322 πN points with 16 parameters has $\chi^2=445$. The fit to 115 $K N$ points with 18 parameters has $\chi^2=145$.

We now discuss several points, under separate headings.

(i) Agreement with Experiment

If the Regge-pole hypothesis is correct, we may perhaps expect the few leading poles to give 90–95% of the scattering amplitude, in the nonasymptotic region considered here. In any case, our simple parameterizations of the t dependence can hardly be more accurate than this. We might therefore expect an

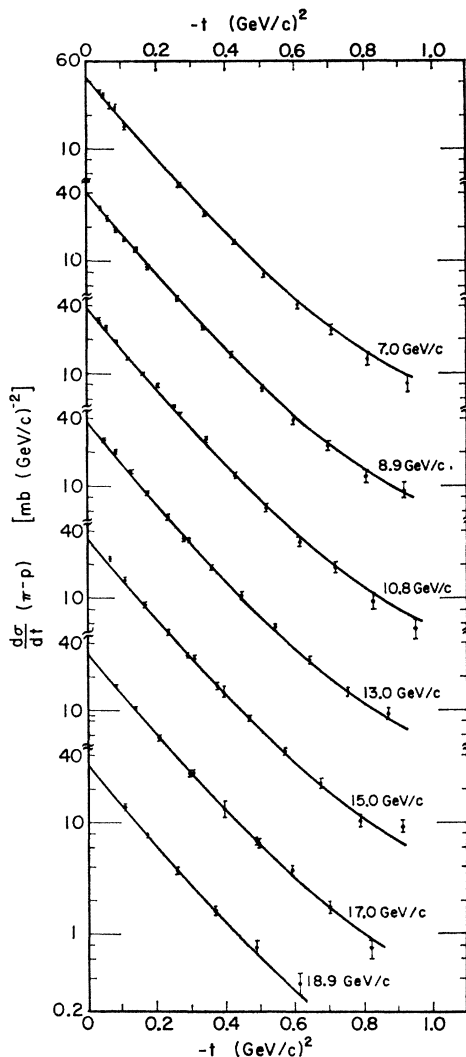


FIG. 3. π^-p differential cross sections at 7, 8.9, 10.8, 13, 15, 17, and 18.9 GeV/c, from Ref. 11, compared with solution 1. Successive sets are spaced by a decade.

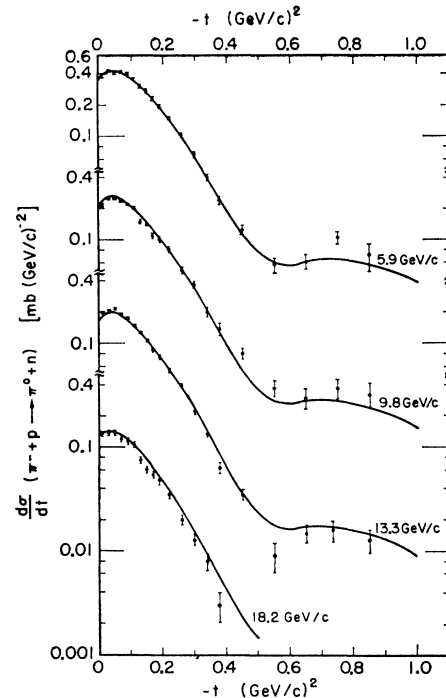


FIG. 4. $\pi^-+p \rightarrow \pi^0+n$ differential cross sections at 5.9, 9.8, 13.3, and 18.2 GeV/c, from Ref. 8, compared with solution 1. The sets of data are spaced by a decade.

accuracy of 10–20% for differential cross sections, but in fact the agreement with experiment is much better than this.

Thus, although the values of χ^2 are not impressive when taken at face value (see Sec. 6), the fit to data is really surprisingly good.

(ii) Parameters of Trajectories

We have given no statistical uncertainties in Tables I through V, since in many cases they would have dubious physical significance. However, there is special interest in the trajectory parameters $\alpha_i(0)$ and $\alpha_i'(0)$.

The statistical standard error on the intercept $\alpha_i(0)$ is typically about 0.002 for ρ , 0.01 for P' , and 0.03 for R and ω . Such a small error for $\alpha_\rho(0)$ is meaningless when compared with systematic differences between solutions.

The intercept $\alpha_P(0)$ has been assumed fixed at 1.0. It is interesting to test this theoretical choice empirically.³³ In solution 2 we varied $\alpha_P(0)$ near 1.0; the χ^2 minimum seemed to lie between 1.0 and 1.005, with a standard error about 0.01.

The standard error on the slope $\alpha_i'(0)$ at $t=0$ is typically about 0.01 for ρ , 0.03 for P and P' , and 0.05 for R and ω . Again, systematic differences are bigger than this for ρ .

It is satisfactory that $\alpha_R(0)$ agrees with the value 0.31 ± 0.05 , deduced by Ahmadzadeh from $N N$ data.²⁰

³³ A suggestion due to H. Lubatti.

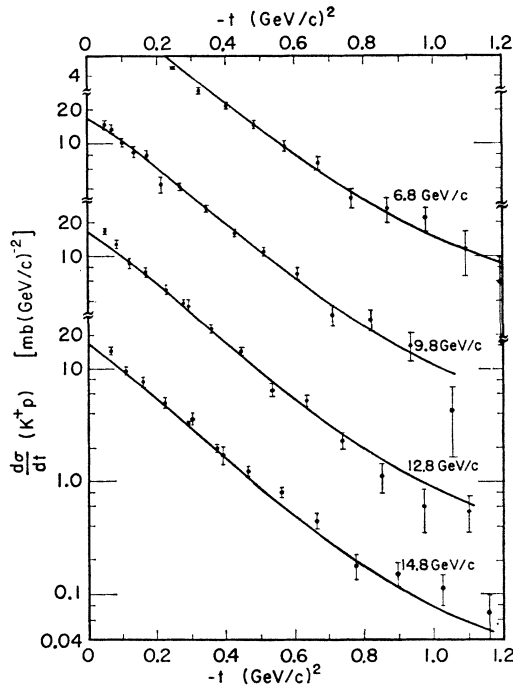


FIG. 5. K^+p differential cross sections at 6.8, 9.8, 12.8, and 14.8 GeV/c from Ref. 11, compared with solution 1. Successive sets are spaced by a decade.

(iii) Slope of ρ Trajectory

There has been great interest in whether the latest πN charge-exchange data^{8,9} really establish a shrinking diffraction peak—i.e., a slope for the ρ trajectory. Logan¹⁰ concluded that they do, using the data of Ref. 9 only. However, to determine an accurate value for the slope he had to assume a straight-line ρ trajectory passing through 1.0 at $t = m_\rho^2$.

Our models give strong evidence for shrinking. We do not require the ρ trajectory to extrapolate to the ρ pole, but we do include a lot of noncharge-exchange data which help to tie down the trajectory. Also we include the more accurate data of Ref. 8.

As a further check, we analyzed the data of Ref. 8

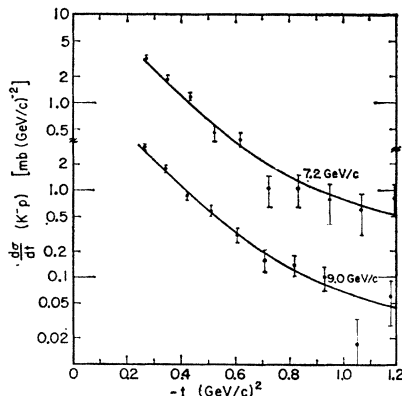


FIG. 6. K^-p differential cross sections at 7.2 and 9.0 GeV/c from Ref. 11, compared with solution 1. The two sets are spaced by a decade.

alone, in terms of the ρ trajectory, following the pattern of solutions 1 and 2. Assuming first a curved trajectory according to Eq. (13), we found the trajectory parameters $\alpha_\rho(0) = 0.540 \pm 0.002$ and $\alpha_\rho'(0) = 0.65 \pm 0.02$. For this fit to data, $\chi^2 = 144$ with 75 data points and 10 adjustable parameters.

Assuming next a *linear* trajectory, instead of the form in Eq. (13), we found a best fit with intercept 0.530 ± 0.003 and slope 0.47 ± 0.02 . For this fit to data, $\chi^2 = 175$, with the same number of points and parameters as before.

The best fit with no shrinking (horizontal trajectory) has intercept 0.45 ± 0.1 and $\chi^2 = 265$.

(iv) Spin Dependence

To determine the spin dependence of πN or KN scattering purely from experiment, polarization and triple-scattering experiments are needed, and they are still lacking. However, the spin dependence of our models is an important help in fitting the data. In particular, the sudden rise in πN charge exchange as

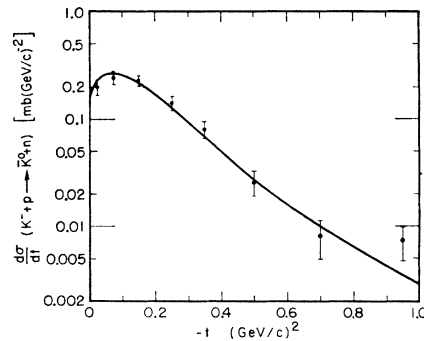


FIG. 7. The $K^- + p \rightarrow \bar{K}^0 + n$ differential cross section at 9.5 GeV/c, from Ref. 7, compared with solution 1.

the scattering angle increases from zero is most naturally explained by a strong spin-flip term—which has to vanish at zero angle—coming from the ρ trajectory.³⁴ The corresponding effect in $\bar{K}N$ charge exchange calls for spin dependence from R as well as from ρ (which is constrained by factorization). Also, spin dependence allows an alternative explanation of the πN crossover effect (Sec. 3).

For a particular model, therefore, there is an optimum spin dependence that gives the best fit to data. But in a broader sense the spin dependence is not really well determined. It may be changed considerably while a 5 to 10% fit to data is still preserved; it may be changed radically if we use a completely different parameterization. For an example, compare solutions 1 and 2 (or 3 and 4), which show how the $B_{P'}$ term may be traded for a change in $A_{P'}$. Also note in the KN case that we

³⁴ The large flip term is adopted as a reasonable physical explanation of the data and is not a special characteristic of Regge poles.

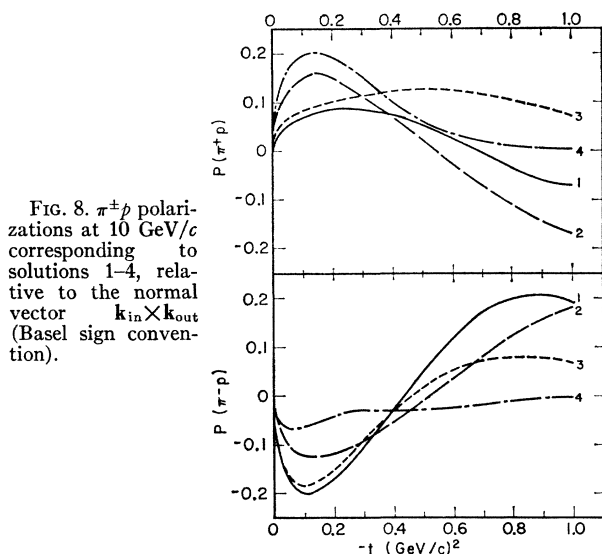


FIG. 8. $\pi^\pm p$ polarizations at 10 GeV/c corresponding to solutions 1-4, relative to the normal vector $\mathbf{k}_{in} \times \mathbf{k}_{out}$ (Basel sign convention).

have not invoked the B_ω term; in fact, a wide range of values are consistent with the data.

The πp polarizations shown in Fig. 8 are therefore illustrations rather than firm predictions. It is interesting to note that the value may be as large as 20% at 10 GeV/c, and that the B_ρ term suggested by the πN charge-exchange data is strong enough to reverse the sign between $\pi^+ p$ and $\pi^- p$ polarization, at some angles. But πN charge-exchange polarization vanishes, of course, since A and B have the same phase when both come from a single trajectory.

Although some parameter freedom remains, polarization data of all kinds would make a valuable test of Regge-pole models.

There is an over-all sign ambiguity for the helicity-flip terms B_i with the data we have. This has been resolved by assuming the ratio A_ρ/B_ρ to have the same sign at $t=0$ as at the ρ pole, $t=m_\rho^2$. It is interesting also to consider the magnitude of this ratio. Taking the $\bar{N}N\rho$ vector and tensor coupling constants to be proportional to the nucleon isovector charge and anomalous moment form factors, we find that $A_\rho/B_\rho \approx 0.2E$ at $t=m_\rho^2$, whereas at $t=0$ the value is $0.08E-0.09E$ for our models. This decrease seems consistent with the fact that, for $t < 0$, A_ρ goes on decreasing faster than B_ρ in these models.

(v) Characteristic of Regge Spin Dependence

A significant feature of the Regge-pole formalism is that the spin dependence of a pole contribution does not vanish asymptotically³⁵—unlike what one expects in a simple diffraction situation. Ordinary (first-rank) polarization vanishes asymptotically only because it

³⁵ As we have defined them, the amplitudes A and B do have different energy dependences. However, their actual contributions to scattering have the same asymptotic dependence: see, e.g., Eq. (2).

happens to require the interference of two amplitudes that are out of phase, and hence requires two poles. However, second-rank polarization effects (e.g., spin correlation, depolarization) can come from a single pole. If the P pole has spin dependence, some of these effects tend asymptotically to nonzero values.

Second-rank polarization measurements at high energy would, therefore, be very interesting. With polarized targets now coming into use, they are not unthinkable.

On this question of the flip and nonflip effects, having the same energy dependence,³⁵ there is already some affirmative evidence in the case of ρ . Assuming the small-angle bump in πN charge exchange is due to, and dominated by, the flip term, we have a measure of its energy dependence. The nonflip term is isolated in charge exchange at $t=0$, and in the total cross-section differences. Our fits to data illustrate that the energy dependences of the flip and nonflip effects are closely comparable.

(vi) Partial-Wave Analysis

Our models offer an interesting contrast to various empirical partial-wave analyses of πN scattering in the multi-GeV region.³⁶⁻³⁸ The latter have generally had to assume a purely imaginary amplitude with no spin dependence³⁹; we have neither of these restrictions.

Table VI illustrates the partial-wave amplitudes for solutions 1 and 2, for $\pi^+ p$ scattering at 10 GeV/c. They are defined by

$$a_{L\pm} = [\exp(2i\delta_{L\pm}) - 1]/i, \quad (25)$$

where $\delta_{L\pm}$ is the (complex) phase shift for orbital

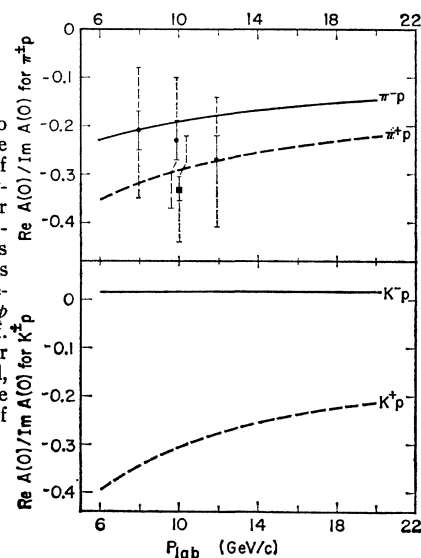


FIG. 9. The ratio of the real to the imaginary part of the forward scattering amplitude for $\pi^\pm p$ and $K^\pm p$ scattering: Solution 1 is shown but the others give very similar predictions. The $\pi^\pm p$ data are from Ref. 40; the inner error bars are statistical, the outer ones are estimated limits of systematic error.

³⁶ S. Minami, Phys. Rev. 133, B1581 (1964).

³⁷ M. L. Perl and M. C. Corey, Phys. Rev. 136, B787 (1964).

³⁸ E. M. Henley and I. J. Muzinich, Phys. Rev. 136, B1783 (1964).

³⁹ A. O. Barut and W. S. Au, Phys. Rev. Letters 13, 489 (1964) have considered adding spin dependence in the lowest waves only.

TABLE VI. Partial-wave amplitudes of solutions 1 and 2 for π^+p scattering at 10 GeV/c.

L	Solution 1				Solution 2			
	$\text{Re}a_{L+}$	$\text{Im}a_{L+}$	$\text{Re}a_{L-}$	$\text{Im}a_{L-}$	$\text{Re}a_{L+}$	$\text{Im}a_{L+}$	$\text{Re}a_{L-}$	$\text{Im}a_{L-}$
0	-0.056	0.224	-0.050	0.248
1	-0.092	0.259	-0.018	0.161	-0.081	0.268	-0.057	0.212
2	-0.098	0.269	-0.033	0.151	-0.078	0.269	-0.040	0.185
3	-0.087	0.257	-0.043	0.143	-0.072	0.257	-0.042	0.162
4	-0.073	0.233	-0.043	0.128	-0.062	0.234	-0.041	0.140
5	-0.060	0.205	-0.037	0.109	-0.051	0.206	-0.038	0.118
6	-0.049	0.176	-0.030	0.088	-0.040	0.175	-0.034	0.096
7	-0.038	0.148	-0.024	0.068	-0.030	0.145	-0.029	0.076
8	-0.029	0.121	-0.019	0.051	-0.023	0.117	-0.025	0.058
9	-0.022	0.098	-0.014	0.036	-0.017	0.092	-0.021	0.043
10	-0.016	0.077	-0.010	0.024	-0.012	0.072	-0.018	0.030
11	-0.012	0.060	-0.007	0.016	-0.009	0.055	-0.015	0.021
12	-0.008	0.045	-0.005	0.009	-0.006	0.040	-0.012	0.014
13	-0.006	0.034	-0.003	0.005	-0.004	0.030	-0.010	0.009
14	-0.004	0.025	-0.002	0.002	-0.003	0.022	-0.008	0.005

angular momentum L and total angular momentum $L \pm \frac{1}{2}$.

The partial-wave analysis was made by continuing the model amplitudes to all scattering angles, well beyond the range where they are fitted to data. However, only the lowest partial waves are sensitive to the wider angles; the higher ones are mainly determined by the forward peak.

Unitarity requires $a_{L\pm}$ to lie within a unit circle in the complex plane, centered at i . In the pure diffraction approximation, $a_{L\pm}$ would be pure imaginary and restricted to lie between 0 and i , the latter corresponding to complete absorption. Notice that the low partial waves in Table VI do not approach complete absorption.

(vii) Phase of the Scattering Amplitude

The phase of the scattering amplitude in our models is not freely disposable, but is determined by the α_i through the signature factors. Where this phase can be measured directly, it offers an important test of this kind of model.⁴⁴

The ratio of the real to the imaginary part of the forward elastic amplitude has been measured for high-energy $\pi^\pm p$ scattering.⁴⁰ The results are shown in Fig. 9, together with the theoretical predictions of solution 1 for $\pi^\pm p$ and $K^\pm p$ scattering (the other solutions all lie within ± 0.01). The models agree with experiment in sign, in magnitude, and in giving a larger value for $\pi^+ p$ than for $\pi^- p$. There have also been various dispersion-relation calculations of this ratio.⁴¹⁻⁴³ The results depend on what asymptotic behavior is assumed for total cross sections, but on the whole they are consistent with experiment and with our models.

The phase of the forward elastic $K^\pm p$ amplitudes

⁴⁰ S. Lindenbaum, rapporteur report to the 1964 International Conference on High Energy Physics at Dubna (to be published).

⁴¹ V. S. Barashenkov and V. I. Dedyu, Dubna report R-1598 1964 (unpublished).

⁴² H. I. Saxer, University of Michigan, Ann Arbor, 1964 (unpublished).

⁴³ G. Hohler, J. Baacke, J. Giesecke, and N. Zovko, Karlsruhe, 1965 (unpublished).

has not yet been measured at high energy. It would be a valuable test.

The phase of the πN forward charge-exchange amplitude is also known. The imaginary part is determined by the total cross-section difference $\sigma_T(\pi^- p) - \sigma_T(\pi^+ p)$ and the optical theorem; the real part then follows from the differential cross section; the two are approximately equal, within a sign. This is an important test of the consistency of the model. In fact, the test is even stronger than this; at $t=0$, A_p is determined by just two parameters, $\alpha_p(0)$ and $C_0(\rho)$. These two successfully account for four independent experimental quantities—the magnitude and the energy dependence of forward charge exchange and the difference of $\pi^\pm p$ total cross sections.

The phase of the $K^- p$ charge-exchange amplitude is also roughly known, from similar arguments. The amplitude appears to be mainly imaginary. The difference between this and the πN situation is neatly explained by the R contribution—the presence of which is required by the total cross sections.²¹ This is another example in which the phase is correctly given by the Regge-pole model.

The other possible charge exchange, $K^+ + n \rightarrow K^0 + p$,

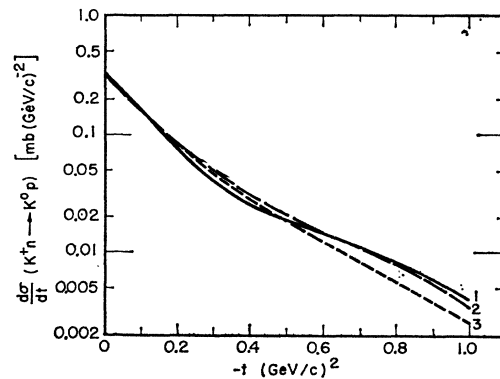


FIG. 10. $K^+ + n \rightarrow K^0 + p$ differential cross sections at 10 GeV/c for solutions 1, 2, and 3.

has not been measured at high energies. The $\rho+R$ Regge-pole model predicts that the forward amplitude is mainly real—i.e., the forward cross section greatly exceeds the optical limit—since the ρ and R terms now change their relative sign, and the real parts add while the imaginary parts cancel.²¹ More specifically, the models we have constructed give predictions for this cross section in the range $|t| < 1$ (GeV/c)², which are illustrated in Fig. 10 at 10 GeV/c. The nonflip term is much stronger there than for $K^-+p \rightarrow \bar{K}^0+n$, giving a bigger cross section and eliminating the dip near $t=0$. Measurements of this process would be very interesting, and would make a good test of the models.

(viii) Second Maximum in πN Charge Exchange

Solutions 1 and 2, which set out to explain the dip and second maximum, do so by making the factor $(1+H) \exp(D_1 t) - H \exp(D_2 t)$ in Eq. (17) change sign, so that B_ρ goes through zero. There are of course other possibilities.

One attractive idea is that B_ρ does indeed go through zero, but because of the kinematical factor α_ρ instead of the other empirical factor in Eq. (17). The curved trajectories we have used, which are rather arbitrarily made to go to $\alpha = -1$ at $t = -\infty$, do not pass through zero in the right region. However, if we assume an almost linear trajectory going through the ρ pole [$\alpha_\rho = 1$ at $t = m_\rho^2 = 0.56$ (GeV/c)²] and through $\alpha_\rho = 0.5$ at $t=0$ (as indicated by much data), it goes through $\alpha_\rho = 0$ near $t = -0.6$ (GeV/c)²—precisely where the dip occurs in πN charge exchange. This is a remarkable coincidence.

To explore this idea, we constructed a model similar to solution 1 but with a linear trajectory of the kind described above and with H lying between 0 and -1 . The resulting fit to wide-angle charge-exchange data was less good, and χ^2 was over 600 for the πN data. However, we believe that an explanation along these lines is tenable.

(ix) Unitary Symmetry

The prediction of SU_3 symmetry is that, in Table IV the coefficients F_0 should be 1 for P and P' , but 0.5 for ρ ; also, the coefficients F should all be zero (see Sec. 5).

These predictions are fulfilled remarkably well for P and ρ ,⁴⁴ but both fail for P' . This may be due to S , the isosinglet member of the R octet, which would contribute with opposite signs to πN and KN amplitudes; if so, it would appear that the contributions of S and the “true” P' are roughly equal in the πN case, for the energy range considered.

Let us also consider the Johnson-Treiman relations

⁴⁴ We remark, however, that F_1 for ρ was constrained to be non-negative.

for forward scattering amplitudes, inferred from the wider SU_6 symmetry⁴⁵:

$$\frac{1}{2}[A(K^+p) - A(K^-p)] = A(K^0p) - A(\bar{K}^0p) \\ = A(\pi^+p) - A(\pi^-p). \quad (26)$$

In terms of our models, if we disregard the small differences between $\alpha_\rho(0)$ and $\alpha_\omega(0)$, this implies

$$\frac{1}{2}[C_0^{KN}(\omega) + C_0^{KN}(\rho)] = C_0^{KN}(\omega) - C_0^{KN}(\rho) \\ = C_0^{\pi N}(\rho). \quad (27)$$

This in turn, when the SU_3 relation for ρ couplings which we have already seen to be verified is used, reduces to

$$C_0^{KN}(\omega) = \frac{3}{2}C_0^{\pi N}(\rho). \quad (28)$$

Comparing Tables II and V, we see this is quite well fulfilled, showing that the data we fit are at least approximately consistent with Eq. (26). A test of lower energy KN and $\bar{K}N$ data has been made previously.⁴⁶

The corresponding relation for helicity-flip amplitudes is irrelevant here, since there are not enough data to fix B_ω and we have arbitrarily set it equal to zero.

Equation (26) would also follow from SU_3 symmetry alone, if ω and ρ belonged to the same octet and had pure F -type coupling to baryons.⁴⁷

(x) Helpful Experiments

Finally we summarize briefly some measurements that would help to test Regge-pole models of the kind we have made: $\pi^\pm p$ polarization, to tie down the spin-flip terms and test the relations between phase and energy dependence ($K^\pm p$ polarization too, of course); $K^+ + n \rightarrow \bar{K}^0 + p$ charge exchange, to test the $\rho+R$ model; $K^\pm p$ Coulomb interference, to test the phase of the forward scattering amplitude; $\pi^- + p \rightarrow \pi^0 + n$ polarization, to see if a single pole really dominates; πN second-rank polarization tensors, to test the Regge characteristics mentioned in (v); $K^- + p \rightarrow \bar{K}^0 + n$ at other energies, to test the energy dependence of the $\rho+R$ model.

ACKNOWLEDGMENTS

We are indebted to Professor Geoffrey F. Chew and Professor Roland Omnes for many valuable discussions about this work, to Dr. Janos Kirz for telling us in advance the Saclay-Orsay results, and to the members of the Theoretical Group for helpful conversations. We thank Dr. David Judd for the hospitality of the Theoretical Group of the Lawrence Radiation Laboratory, where this work was done.

⁴⁵ K. Johnson and S. B. Treiman, Phys. Rev. Letters 14, 189 (1965).

⁴⁶ R. Good and N. Xuong, Phys. Rev. Letters 14, 191 (1965).

⁴⁷ R. F. Sawyer, Phys. Rev. Letters 14, 471 (1965).